






Carrier Frequency Offset Estimation in the Eigenvalue Domain

Takaya Maeda , Daisuke Hisano , *Member, IEEE*, Yuki Yoshida , *Member, IEEE*, Akihiro Maruta , *Member, IEEE, Member, OSA*, and Ken Mishina , *Member, IEEE*

Abstract—Optical eigenvalue transmission is a promising technique to overcome Kerr nonlinear limits in optical communication systems. The optical eigenvalue associated with the nonlinear Schrödinger equation is invariant during fiber-based nonlinear dispersive transmission. However, the effect of carrier frequency offset (CFO) induces an eigenvalue shift in the presence of the CFO for digitally coherent receivers. The CFO estimation method using eigenvalues capable of achieving highly accurate estimations and can be applied to an eigenvalue transmission system has been proposed. However, a detailed analysis of the eigenvalue-based CFO estimation method is yet to be examined. This study examines the estimation accuracy and limitations of the CFO estimation method through numerical simulations and experiments. The eigenvalue-based method achieves estimation accuracy of less than 10 kHz when the time window size $W = 6.4$ ns and sampling rate $R_s = 20$ GSa/s in numerical simulations. Moreover, the estimation error is proportional to energy loss when the time window size W and sampling rate R_s are limited. Through experiments, we achieve a fine estimation accuracy below 1 MHz when $W = 12.8$ ns and $R_s = 5$ GSa/s, although the accuracy is limited by the noise effect.

Index Terms—Eigenvalue modulation, carrier-frequency offset (CFO), optical soliton.

I. INTRODUCTION

OPTICAL eigenvalue communication [1] based on inverse scattering transform (IST) [2] is a promising technology to overcome the Kerr nonlinear limit in fiber-optic communications. IST is a well-known nonlinear Fourier transform (NFT). The eigenvalues of the equation associated with the nonlinear Schrödinger equation (NLSE) are invariant during propagation in nonlinear dispersive lossless fibers although the waveform and frequency spectrum change. Accordingly, Hasegawa and Nyu

proposed the concept of eigenvalue communication in 1993 [1]. The concept of advanced communication has attracted renewed attention following the remarkable developments in coherent digital technology, which enables the detection of eigenvalues and scattering parameters in real systems [3], [4]. Recently, many studies on eigenvalue communication have been conducted [5]. To increase transmission capacity, multi-eigenvalue transmission [6], [7], [8] and multilevel modulation methods using a nonlinear spectrum or scattering coefficient b [9], [10] have been demonstrated. Furthermore, several studies on neural network-based demodulation methods of eigenvalue-modulated signals to improve the receiver sensitivity and extend the transmission distance have been reported [11], [12].

Eigenvalue communication systems utilized a digital coherent receiver to obtain the complex envelope amplitude of optical signals and to detect the eigenvalues and scattering coefficients. Carrier frequency offset (CFO) estimation is essential to estimate and compensate for the wavelength mismatch between the carrier signal and local oscillator (LO) in the digital coherent receiver, which can reach ± 5 GHz with a micro-ITLA [13], [14], [15] because CFO induces an eigenvalue shift and symbol error [5], [16]. In general feedforward digital signal processing, the CFO is estimated and compensated for before phase estimation.

Several CFO estimation methods, such as algorithms using the spectrum in the frequency domain (FD) for general quadrature amplitude modulation (QAM) Systems have been proposed [17], [18], [19], [20]. In [17], [18], an algorithm using the periodogram of the 4th power of a received QAM signal was utilized to achieve blind CFO estimation with a wide frequency range and high estimation accuracy. In [19], the CFO was estimated using an FFT-based method without removing the phase of the modulated data. A wide range and modulation formats Independent estimation method using a digital pilot have been proposed [20]. However, frequency-spectrum-based methods require numerous samples to achieve highly accurate CFO estimation.

In contrast, a CFO estimation method using eigenvalues obtained using NFT or nonlinear spectra has been reported [16], [21]. This method detects soliton components of optical pulses and estimates the CFO from soliton frequencies; thus, it can achieve highly accurate estimation with fewer samples. Furthermore, this method is effective for different transmission distances because the pulse shape of the fundamental soliton and its eigenvalues are invariant during transmission. In addition, NFT-based methods can be applied to both QAM

Manuscript received 15 April 2023; revised 22 June 2023; accepted 26 June 2023. Date of publication 28 June 2023; date of current version 2 November 2023. This work was supported in part by Beyond 5G R&D Promotion Project under Grant 01401 and in part by the National Institute of Information and Communications Technology (NICT), Japan. (*Corresponding author: Ken Mishina.*)

Takaya Maeda, Daisuke Hisano, Akihiro Maruta, and Ken Mishina are with the Graduate School of Engineering, Osaka University, Suita 565-0871, Japan (e-mail: maeda@pn.comm.eng.osaka-u.ac.jp; hisano@comm.eng.osaka-u.ac.jp; maruta@comm.eng.osaka-u.ac.jp; mishina@comm.eng.osaka-u.ac.jp).

Yuki Yoshida is with the Graduate School of Engineering, Osaka University, Suita 565-0871, Japan, and also with the National Institute of Information and Communications Technology (NICT), Koganei, Tokyo 184-8795, Japan (e-mail: yuki@nict.go.jp).

Color versions of one or more figures in this article are available at <https://doi.org/10.1109/JLT.2023.3290484>.

Digital Object Identifier 10.1109/JLT.2023.3290484

and eigenvalue communication systems. However, a detailed analysis of the NFT-based method is yet to be conducted.

This study numerically and experimentally investigates an NFT-based carrier frequency estimation method in the eigenvalue domain (ED). As an extension of our previous study [22], [23], we examine the CFO estimation method in detail and further investigated the generalized characteristics, including the effects of time window size, sampling rate, eigenvalue, analog-to-digital (A/D) conversion, and noise. In addition, the limitations of the estimation in practical applications are analyzed through experiments. In the simulation, the NFT-based method achieved a high-accuracy CFO estimation with no other fitting except NFT. The NFT-based CFO estimation method achieve an estimation accuracy of less than 10 kHz under the appropriate condition of the time window size and sampling rate in the numerical simulations. In addition, we indicate that the estimation error is proportional to energy loss when the time window size and sampling rate are limited. Through experiments, a fine estimation accuracy below 1 MHz is demonstrated, although the accuracy was limited by the noise effect.

The remainder of this article is organized as follows. Section II describes eigenvalue communication based on the NFT and CFO estimation methods in the ED. Section III discusses the results of numerical simulations. Section IV discusses the experimental results to demonstrate the limiting factors and achievable estimation accuracy of the NFT-based CFO estimation. Finally, Section V concludes the study.

II. NFT-BASED CFO ESTIMATION METHOD

A. Eigenvalue Communication

The behavior of the complex envelope amplitude of a light wave propagating in an optical fiber is described as follows: [24]

$$i\frac{\partial E}{\partial z} - \frac{\beta_2}{2}\frac{\partial^2 E}{\partial t^2} + \gamma|E|^2E = -i\alpha E, \quad (1)$$

where z , t , $E(z, t)$, β_2 , γ , and α are the propagation length, time, complex envelope amplitude of the electric field, group velocity dispersion, nonlinear parameter, and fiber loss, respectively. We considered a transmission channel in which the amplifier spacing was sufficiently larger compared with the dispersion length in an anomalous dispersion regime. In this case, the loss effect is negligible and (1) can be transformed into the normalized form of the NLSE, as follows: [25]

$$i\frac{\partial u}{\partial Z} + \frac{1}{2}\frac{\partial^2 u}{\partial T^2} + |u|^2u = 0, \quad (2)$$

where Z , T , and u are the normalized propagation length, time, and electric field, respectively. The eigenvalue equation associated with (2) is as follows:

$$\frac{\partial \phi_1}{\partial T} = -i\zeta\phi_1 + iu\phi_2, \quad \frac{\partial \phi_2}{\partial T} = iu^*\phi_1 + i\zeta\phi_2, \quad (3)$$

where ζ and ϕ_l ($l = 1, 2$) are the complex eigenvalues and eigen function, respectively. Provided $u(T, Z)$ satisfies (2), the eigenvalue ζ is invariant with respect to Z .

Various multi-level modulation schemes that use eigenvalues have been proposed. A 2^N -ary multi-level modulation signal using the on-off states of multiple eigenvalues ζ_n was proposed [6], [7], [8]. A 4096-ary eigenvalue-modulated signal using 12 eigenvalues was reported [8]. Another QAM-based modulation scheme, which varies the amplitude and phase of the scattering parameter or nonlinear spectra, was proposed [9], [10]. In these modulation schemes, coding was performed at the transmitter to assign bit sequences to the patterns of the eigenvalues ζ or scattering parameters $b(\zeta)$. Subsequently, solitons corresponding to the eigenvalues ζ or scattering parameters $b(\zeta)$ were generated and the soliton pulse train was transmitted as an optical signal to the fiber. At the receiver, the eigenvalues ζ and scattering parameters $b(\zeta)$ were detected from the complex envelope amplitude of the received soliton. Consequently, the detected pattern was decoded into a bit series. In these modulation schemes, the eigenvalue ζ is constant regardless of the propagation length and the scattering parameter $b(\zeta)$ evolves linearly with the propagation length. Therefore, these modulation schemes are not influenced by the nonlinear distortion and are expected to be promising technologies to overcome the nonlinear Kerr limit. However, in the presence of the CFO, the CFO effect must be estimated and compensated for because the CFO induces eigenvalue shifts and errors in pattern identification.

B. CFO Estimation Method

The CFO is estimated by measuring soliton frequencies between the transmitted and received soliton pulses in the NFT-based methods. In the case of a soliton pulse with one eigenvalue ζ given by $\zeta = (\kappa + i\eta)/2$, where κ and η (> 0) are arbitrary real numbers, 1-soliton solution $u(Z, T)$ with a single eigenvalue is expressed as follows:

$$u(Z, T) = \eta \operatorname{sech}[\eta(T + \kappa Z)] \exp\left(-i\kappa T + i\frac{\eta^2 - \kappa^2}{2}Z\right), \quad (4)$$

where position T_0 and phase ϕ_0 of the soliton peak at $Z = 0$ are set to zero. In (4), the phase of the soliton pulse varies with time T , using $-\kappa T$. That is, the frequency shift in the received pulses appears as a shift in the real part of the eigenvalue $\operatorname{Re}[\zeta] = \kappa/2$ in the ED. Conversely, the imaginary part of the eigenvalue $\operatorname{Im}[\zeta] = \eta/2$ represents the amplitude and pulse width of the soliton pulse. The relationship between the frequency offset f_{offset} and eigenvalue shifts is expressed as follows:

$$u(T) \exp(-i2\pi f_{\text{offset}} t_0 T) \Leftrightarrow \zeta - \pi f_{\text{offset}} t_0, \quad (5)$$

where t_0 is the base time for signal generation that satisfies $T = t/t_0$ for real time t . An overview of the CFO estimation method in ED is shown in Fig. 1. Based on the relationships in (5), the CFO can be estimated by calculating the difference between the real parts of the eigenvalues of the transmitted and received soliton pulses. The estimated CFO \hat{f}_{offset} is expressed as follows:

$$\hat{f}_{\text{offset}} = \frac{\operatorname{Re}[\zeta_t] - \overline{\operatorname{Re}[\zeta_r]}}{\pi t_0}. \quad (6)$$

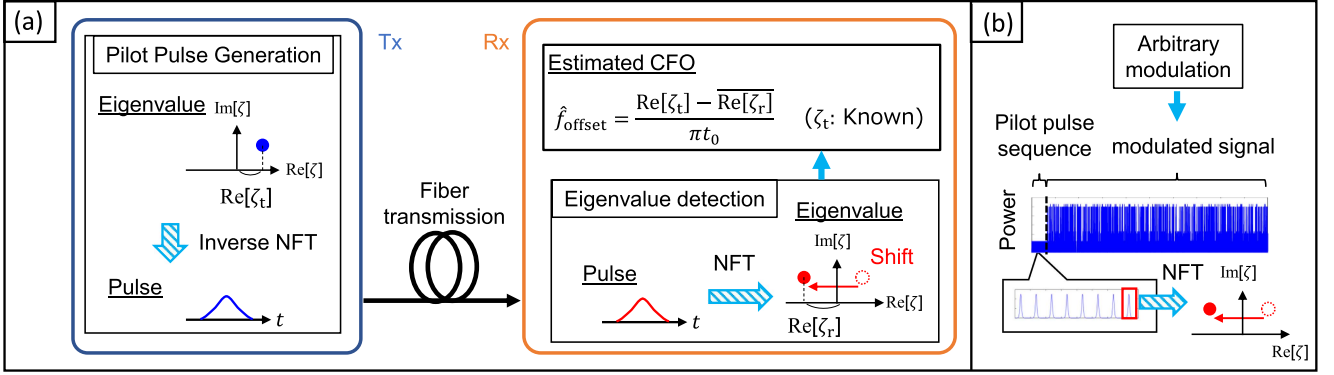


Fig. 1. NFT-based CFO estimation method.

When the real parts of the eigenvalues of the transmitted pulses are zero, the CFO is calculated by referring only to the eigenvalues of the received pulses. Suppose the estimation accuracy is limited by noise. In that case, the estimation accuracy can be improved by calculating the average of the eigenvalues detected from multiple received pulses. The CFO estimation and compensation can be achieved by periodically transmitting and receiving known pilot soliton pulses when the CFO fluctuation speed is sufficiently slower than the modulation rate, as shown in Fig. 1. In addition, because the eigenvalues are invariant during the fiber propagation, the same process as the estimation method can be applied even for different transmission distances.

The proposed CFO estimation method has the potential to be applied to an advanced estimation without pilot pulses to achieve a higher spectral efficiency. However, the algorithm depends on the modulation format of the eigenvalue communication. For example, in b -modulation, a specified eigenvalue that varies the scattering parameter b is transmitted. The proposed CFO estimation method can be applied without pilot pulses because the transmitted eigenvalue is known in the b -modulation. However, a CFO estimation for the on-off encoding of multi-eigenvalue requires a complicated algorithm because the number of the transmitted eigenvalue depends on the bit pattern. In this study, we focus on investigating the fundamental characteristics of the proposed CFO estimation method by assuming the use of the pilot pulses.

In addition, we compare the NFT-based method with the FFT-based estimation method in the FD [17]. Various CFO estimation methods have been proposed to achieve a high estimation accuracy [17], [18], [19], [20], however, additional fittings and processing to the FFT-based method are involved in these methods, which increase the computational complexity and required memory size. Therefore, we employed the following FFT-based method as a standard of comparison, which can simply compare the performance of CFO estimation between two transforms, the FFT and NFT. In the FFT-based method, CFO was estimated by calculating the difference in the peak frequency between the transmitted and received pulse sequences. The estimated CFO was calculated as follows:

$$\hat{f}_{\text{offset}} = \arg \max_f \left| \sum_t E_f(t) e^{-i2\pi ft} \right|^2$$

$$- \arg \max_f \left| \sum_t E(t) e^{-i2\pi ft} \right|^2, \quad (7)$$

where E_f is the soliton pulse sequence influenced by the CFO. The accuracy of CFO estimation depends on the window size of the FFT because this method refers to the frequency spectrum calculated using the FFT.

III. NUMERICAL SIMULATIONS

A. Simulation Model

We investigated the CFO estimation accuracy of the NFT-based method through simulations. The simulation model is shown in Fig. 2. CFO estimation was performed using fundamental soliton pulses with eigenvalues on the imaginary axis ($\text{Re}[\zeta_t] = 0$). First, the eigenvalues were converted into soliton pulses and transmitted as optical pulses using an IQ modulator. White Gaussian noise was added to the communication channel and optical pulses were received by a coherent receiver for the back-to-back configuration. The CFO at the receiver varied from -5 to 5 GHz. Eigenvalues were detected from the received pulses using the Fourier collocation method [3], [26]. NFT-based CFO estimation was performed based on the procedure described in the previous section. In the simulation, we considered an ideal transmitter and receiver with flat frequency characteristics. Only the sampling rate limited the spectral bandwidth. The soliton pulse was generated at the transmitter under the specified sampling rate and the pulse was received at the receiver without distortion.

The absolute value of the difference between the estimated and actual CFO was defined as the estimation error for evaluating the estimation accuracy. The estimation accuracy was evaluated by varying the imaginary part of the eigenvalue ($\text{Im}[\zeta]$), time window size W , and sampling rate R_s . The base time t_0 was set to 50 ps. Moreover, FFT-based CFO estimation was performed to compare the estimation accuracy with that of the NFT-based estimation method.

B. Simulation Results

1) *Basic Characteristics*: First, we examined the results without noise loading to discuss the characteristics of ideal CFO

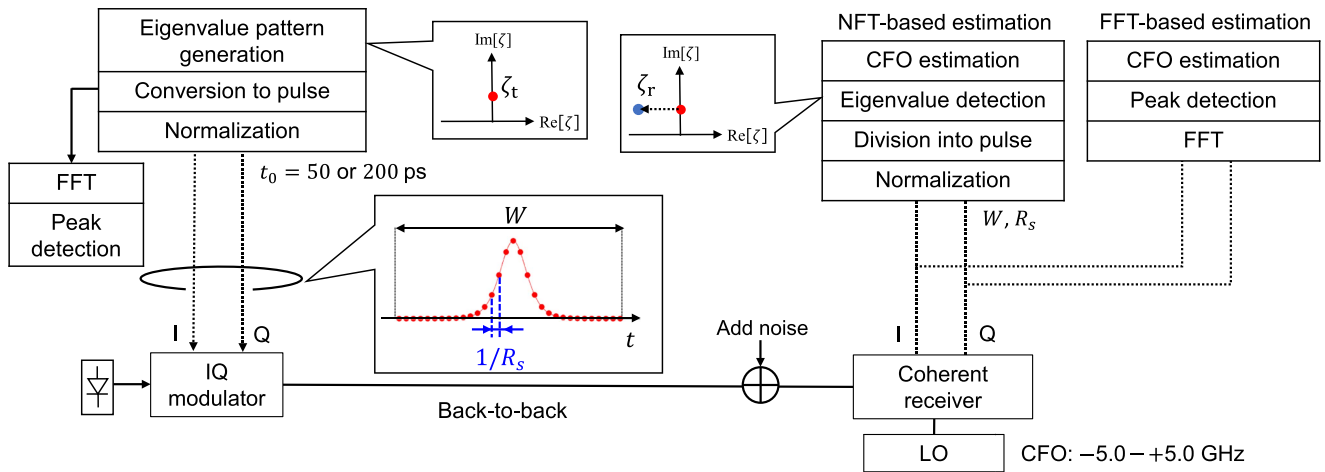


Fig. 2. Simulation model.

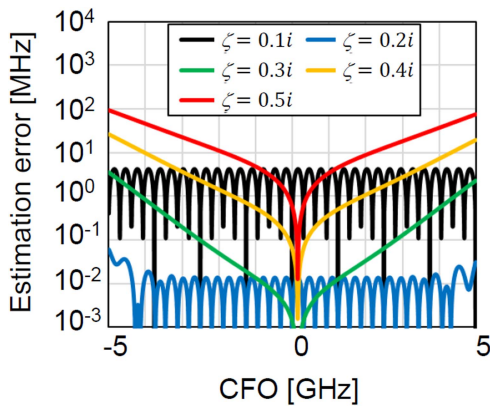


Fig. 3. CFO dependence of estimation error.

estimation in the ED. The CFO was estimated from one soliton pulse ($N_p = 1$) under noiseless conditions. The estimation error obtained by varying the CFO and $\text{Im}[\zeta]$ for $W = 3.2$ ns and $R_s = 20$ GSa/s is shown in Fig. 3. For $\zeta = 0.1i$ and $0.2i$, the estimation errors change periodically with the CFO value. This result originated from the eigenvalue detection of the Fourier collocation method and the period corresponded to an FFT resolution of 0.3125 GHz ($=1/W$). The estimation accuracy was limited by the time window size under these conditions. In contrast, for eigenvalues $\zeta = 0.3i, 0.4i$, and $0.5i$, the estimation error increased with the CFO. This phenomenon resulted from an eigenvalue shift owing to bandwidth limitations. The soliton pulse cannot be detected exactly by NFT in the case of the W or R_s limitations, which resulted in a CFO estimation error.

The result of eigenvalue detection at $W = 3.2$ ns and $R_s = 20$ GSa/s is shown in Fig. 4 when the amount of frequency shift varied. The range of detectable eigenvalues was restricted when the sampling rate was limited. Moreover, the eigenvalue shifted significantly when the frequency shift was large and the imaginary part of the eigenvalue was large. The pulse waveforms and spectra when the imaginary part of the eigenvalue varied are shown in Fig. 5. The solid lines represent the spectra with a bandwidth limit of $R_s = 20$ GSa/s and the dotted lines represent

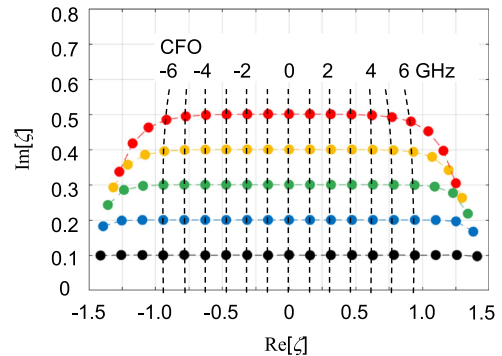


Fig. 4. R_s limitation.

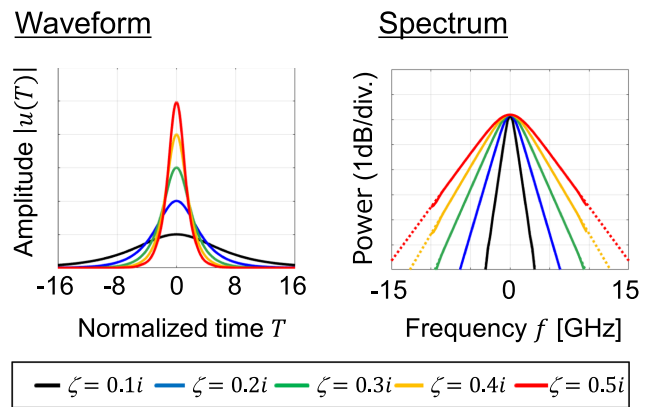


Fig. 5. Time waveform and spectrum.

the ideal spectra of the soliton. When the imaginary part was large, the amplitude of the soliton pulse was larger and its spectral width was wider. However, when the imaginary part was small, the pulse width of the soliton pulse widened, and the spectral width narrowed. Therefore, when the time window size W and sampling rate R_s were limited, the pulse waveform and spectrum of the soliton pulse were finitely terminated, which resulted in a shift in the eigenvalues detected by NFT and the CFO estimation errors.

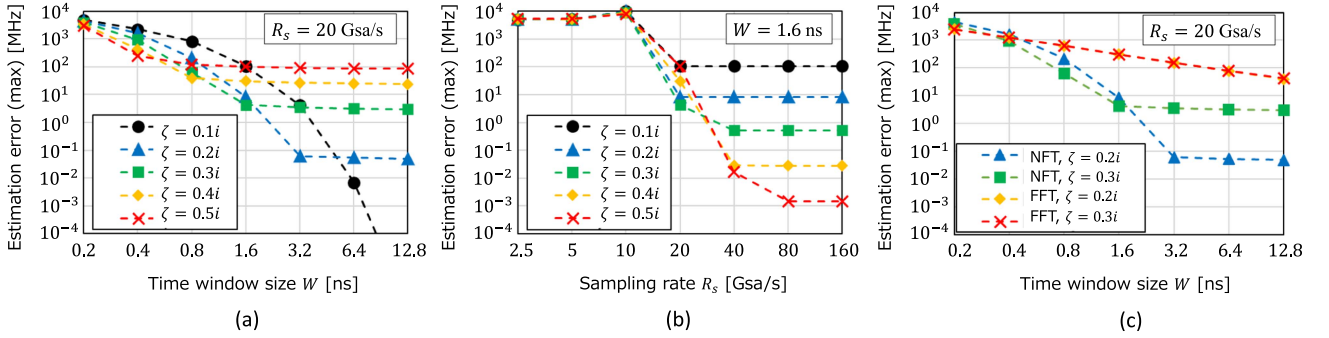


Fig. 6. CFO estimation error (a) W dependence, (b) R_s dependence, (c) Comparison with the FFT-based estimation.

The maximum values of estimation errors obtained by varying W and R_s are shown in Fig. 6(a) and (b), respectively. The maximum estimation errors between the CFO from -5 to 5 GHz are plotted in Fig. 6. The estimation error decreased with increasing W and R_s . When R_s was fixed, the estimation accuracy was limited by R_s even for large window sizes, as shown in Fig. 6(a). The bandwidth limitation by the sampling rate degrades the estimation accuracy. This result implies that bandwidth limitations and frequency characteristics of electrical/optical components degrade the estimation accuracy. In contrast, the estimation error was determined by W for a fixed value of W , as shown in Fig. 6(b).

The maximum estimation errors compared with the FFT-based estimation method in FD are shown in Fig. 6(c) [17]. Moreover, the estimation error in the FD decreased with increasing W ; however, it does not change with the imaginary part of the eigenvalue $\text{Im}[\zeta]$. The NFT-based CFO estimation method demonstrated a higher estimation accuracy compared with the FFT-based method for W from 0.8 to 12.8 ns. The FFT-based method can achieve a higher estimation accuracy by increasing the window size W to more than 12.8 ns because the resolution of the spectrum depends on the FFT window size. However, this estimation has a high computational complexity and requires a longer monitoring time. For example, a window size of 204.8 ns and 4096 sampling points are required to achieve comparable accuracy with the NFT-based method for $\zeta = 0.3i$ in Fig. 6(c). The NFT-based method, which detected an eigenvalue as a soliton component, can achieve fine CFO estimation without additional fittings.

Regarding the computational complexity, the NFT-based method requires the number of flops of $\mathcal{O}(N_s^3)$, where N_s indicates the number of sampling points, for the eigenvalue detection using the Fourier collocation method. On the other hand, the FFT-based method requires $\mathcal{O}(N_s \log_2 N_s)$ flops for FFT. To achieve an estimation accuracy of approximately 3 MHz, as shown in Fig. 6(c), the required number of sampling points are 64 and 4096 for the NFT- and FFT-based methods, respectively. Thus far, the total computational complexity of the NFT-based method is higher than that of the FFT-based method. However, several algorithms have been proposed to reduce the computation complexity and time for eigenvalue detection [5], [27]. Computational complexity reduction and accuracy investigation

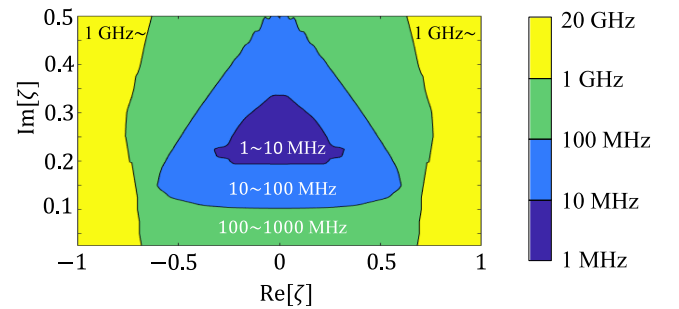


Fig. 7. ζ dependence of the estimation error.

using a fast algorithm for eigenvalue detection need to be studied further.

Fig. 7 shows the estimation accuracy when the real $\text{Re}[\zeta]$ and imaginary parts $\text{Im}[\zeta]$ of ζ are changed, under the assumption that W and R_s are limited by the system configuration. A contour plot of the maximum estimation error when ζ was varied at $W = 1.6$ ns and $R_s = 20$ Gsa/s is shown in Fig. 7. An estimation error of less than 10 MHz was achieved when $\text{Re}[\zeta] = 0$ and $\text{Im}[\zeta] = 0.25$. In NFT-based CFO estimation, the eigenvalue dependence of the estimation accuracy varied with W and R_s . Therefore, the estimation accuracy can be improved by using appropriate eigenvalues on the real axis, depending on the magnitudes of W and R_s . In other words, the result shown in Fig. 7 indicates that the optimum eigenvalue ζ can be determined when W and R_s are limited by the system configuration.

Second, we investigated the characteristics of the estimation error during normalization. The maximum estimation errors between CFO from -5 to 5 GHz are plotted as shown in In Fig. 8(a). The horizontal axis represents the normalized W using the full width at half maximum (FWHM) of the pulse because the pulse width differs according to the eigenvalue. In Fig. 8(b), the CFO was provided from $-5r$ to $5r$ GHz for normalization. r is the ratio of δ_0/δ_ζ , where δ_0 is the basic FWHM of the spectrum for $\zeta = 0.3$ and δ_ζ is the FWHM of the spectrum for ζ in CFO estimation. The horizontal axis represents the normalized R_s using the FWHM_f of the spectrum. The estimation error decreased with increasing W and R_s . However, similar values of the estimation error were obtained, even for different eigenvalues during normalization. The time window size of the

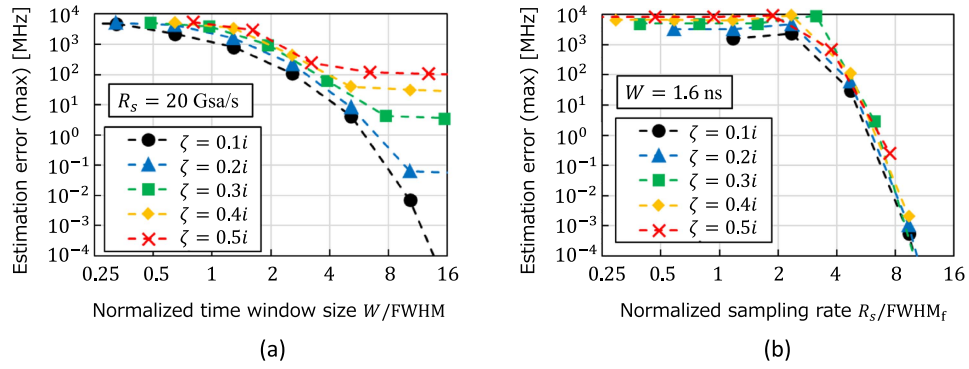


Fig. 8. CFO estimation error (a) normalized W dependence, (b) normalized R_s dependence.

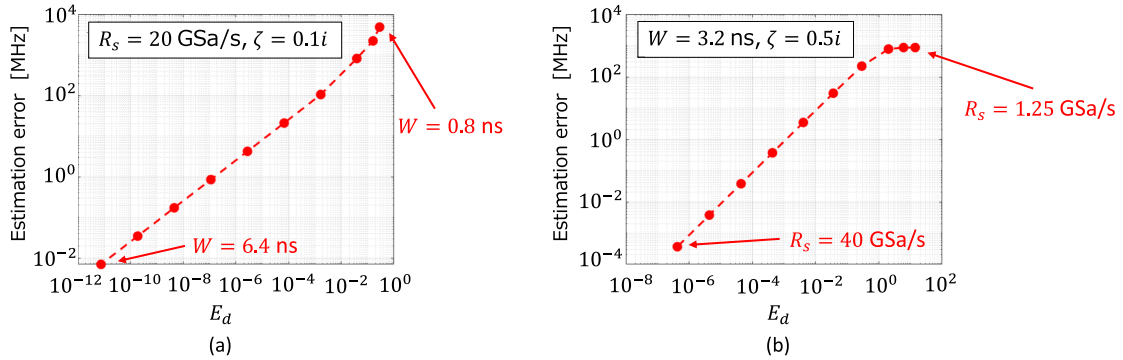


Fig. 9. E_d dependence on the CFO estimation error (a) W varied and (b) R_s varied.

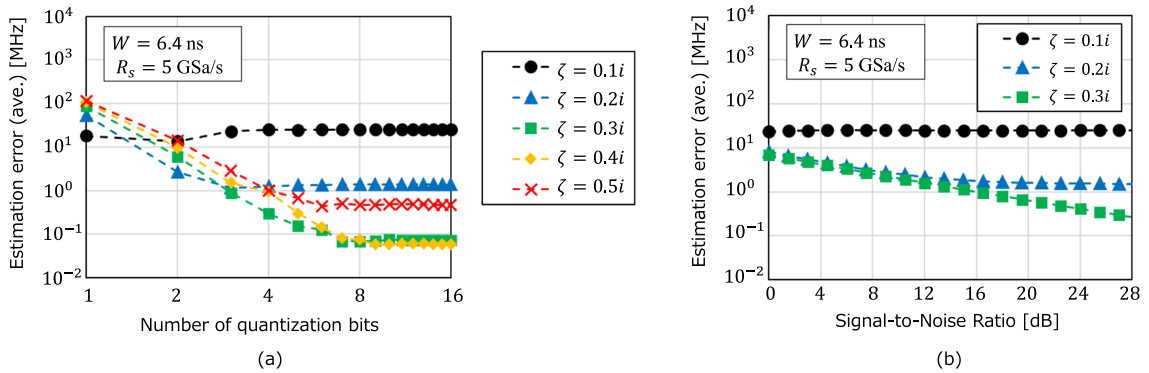


Fig. 10. (a) Effect of quantization and (b) effect of noise.

sixfold FWHM and the bandwidth of the sixfold FWHM of the spectrum are required to achieve the CFO estimation accuracy below 10 MHz.

In addition, we discuss the relationships between the estimation error and energy loss. A soliton with eigenvalue is a hyperbolic secant pulse that includes energy for $|t| \rightarrow \infty$ and $|f| \rightarrow \infty$. We observed a soliton pulse with a limited time window size and bandwidth when CFO estimation was performed even in the simulation. We considered the energy difference $E_d = |E_i - E_l|$, where E_i and E_l are the energies of the ideal and limited solitons for CFO estimation, respectively. The E_d dependence on CFO estimation error when W and R_s varied is shown in Fig. 9. The estimation error was proportional to the energy difference E_d . When the time window size W and the

sampling rate R_s were limited, the estimation error was limited by the energy loss from the ideal soliton.

2) *Effects of Quantization and Noise:* In practical systems, the received signal is distorted owing to system impairments, such as optical amplifier noise, receiver noise, and quantization. We investigated the effect of quantization and noise on estimation accuracy. In this simulation, the following parameters were adopted: $W = 6.4$ ns, $R_s = 5$ Gsa/s, $t_0 = 200$ ps, and CFO of -120 MHz. The estimation error was measured as the average of the absolute values of the errors after ten estimation iterations. The estimation was performed using 32 soliton pulses. The estimation error obtained by varying the number of quantization bits at the receiver is shown in Fig. 10(a). The larger the number of quantization bits, the better the accuracy. When the number of

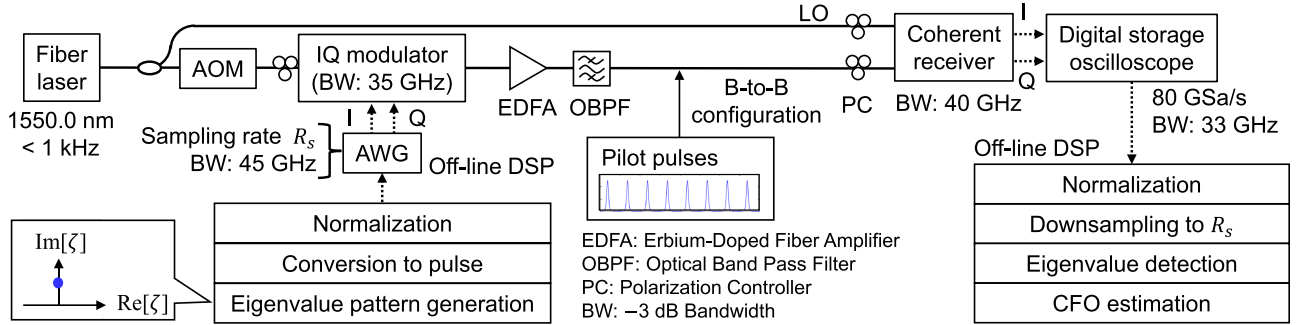


Fig. 11. Experimental setup.

quantization bits is sufficiently large, the estimation accuracy is limited by W or R_s . Finally, four and seven bits were required to achieve estimation accuracy below 1 and 0.1 MHz, respectively. The estimation error obtained by varying the OSNR is shown in Fig. 10(b). We assumed that white Gaussian noise was added to the optical amplifier in this simulation. The OSNR should be maintained above 16 dB for $\zeta = 0.3$ to achieve an estimation error below 1 MHz. The estimation accuracy is limited by noise for $W = 6.4$ ns, R_s 5 GSa/s, and $\zeta = 0.3$ when we apply the NFT-based CFO estimation to the system with quantization bits of 8 and SNR from 16 to 28 dB.

In this simulation, we investigated the effect of noise on the estimation accuracy for the B-to-B configuration. On the other hand, amplified spontaneous emission (ASE) noise from optical amplifiers is accumulated through a long-haul transmission in a real communication system. When the SNR is degraded by the ASE noise, the effect on the estimation error can be seen in Fig. 10(b). In addition to the SNR degradation, it is well-known that a timing jitter occurs in the soliton transmission when the ASE noise is accumulated [28]. Provided that the waveform of a soliton is captured with a sufficiently large time window size at a receiver, the eigenvalue is not affected by the timing jitter. However, when the window size W is limited, the timing jitter induces an energy loss E_d from the pulse tail, which leads to an increase in the estimation error.

At the end of the simulation, an example of the procedure for optimizing the parameters of the proposed method to obtain the most accurate CFO estimation is described. As shown in Fig. 10(b), an estimation accuracy using an eigenvalue with a small imaginary part is limited by the noise effect and time window size W . Although the noise effect can be reduced by increasing the number of pulses, it decreases the net bit rate (spectral efficiency) and increases the computational complexity. Additionally, an eigenvalue with a large imaginary part requires a wide bandwidth and high sampling rate to obtain a high estimation accuracy. An example of the optimization is as follows: From the system configuration, the available time window size W , sampling rate R_s , number of pilot pulses, computational resource, number of quantization bits, and noise level (SNR) are determined. Under the condition of limited W and R_s , the candidates of eigenvalues ζ can be selected from Fig. 6. For example, an eigenvalue range of an imaginary part $\zeta = 0.2i - 0.4i$ is the candidate when the maximum W and

R_s are 1.6 ns and 20 GSa/s, respectively. Consequently, the optimum eigenvalue can be found by simulating the estimation using several eigenvalues between $\zeta = 0.2i$ and $\zeta = 0.4i$ under the specified condition of the system, such as the number of pilot pulses, number of quantization bits, and SNR, as shown in Fig. 7

IV. EXPERIMENT

A. Experimental Setup

We investigated the CFO estimation accuracy of the NFT-based method through experiments for back-to-back operations. The experimental setup is shown in Fig. 11. A shared lightwave source was used for the signal light and LO to obtain a static CFO. An acoustic optical modulator introduced a static frequency shift of 119.995 MHz on the signal measured using the periodogram method with a long measurement time of 100 μ s. An optical soliton pulse was generated using an arbitrary waveform generator and IQ modulator with a base time of $t_0 = 200$ ps. A fundamental soliton with an eigenvalue on the imaginary axis ($\text{Re}[\zeta] = 0$) was used as the pilot pulse. The optical soliton pulse was received by a coherent receiver and A/D conversion was performed using a digital storage oscilloscope (DSO) at 80 GSa/s with 8 bits of quantization. The CFO was estimated using the NFT-based method. The estimation accuracy was evaluated by varying the imaginary part of the eigenvalue ($\text{Im}[\zeta]$), time window size W , sampling rate R_s , and number of pulses N_p . The pulse duration was calculated as $t_0 \times W$.

B. Experimental Results

The average estimation errors obtained by changing W and R_s for $N_p = 32$ are shown in Fig. 12(a) and (b), respectively. The estimation error was measured as the average of the absolute error values after 10 iterations. The estimation error decreased with an increase W or R_s . The trends of the experimental results correspond to those of the simulation results (as discussed in the previous section). When W and R_s were sufficiently large, the estimation accuracy was limited by experimental factors, such as the noise and resolution of the A/D conversion. The estimation error obtained by changing the number of pulses N_p for $W = 6.4$ ns and $R_s = 5$ GSa/s is shown in Fig. 12(c). When $\zeta = 0.1i$, the estimation accuracy remained unchanged even when N_p was increased. This is because the estimation

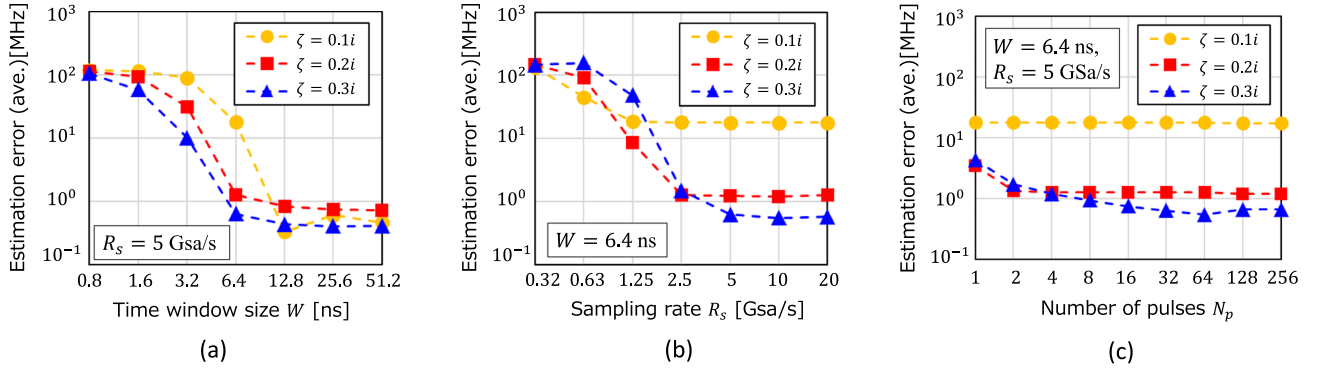


Fig. 12. Experimental results: (a) W dependence, (b) R_s dependence, (c) N_p dependence.

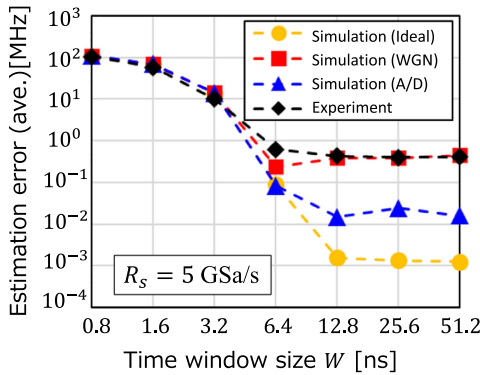


Fig. 13. Comparison with the simulation results.

accuracy was limited by the window size W , not the noise effect, under the condition of $W = 6.4$ ns, as shown in Fig. 12(a). On the other hand, for $\zeta = 0.2i$ and $\zeta = 0.3i$, the estimation error decreased as N_p increased. When N_p was sufficiently large, the estimation error converged to a certain level, which was limited by a window size W of 6.4 ns, as shown in Fig. 12(a). The NFT-based method, which detects an eigenvalue as a soliton component, could achieve a fine CFO estimation in the order of megahertz (5.3–6.4 MHz) even with one pilot pulse (pulse duration: 6.4 ns). When $W = 12.8$ ns, $R_s = 5$ Gsa/s, and $N_p = 32$, a fine accuracy below 1 MHz was achieved even in the experiments.

Next, we discussed the estimation accuracies of the experiments compared with those of the numerical simulations. We performed the numerical simulation using a base time $t_0 = 200$ ps and CFO of 119.189 MHz to match the experimental conditions. The comparison with the simulation results is shown in Fig. 13. The parameters of $\zeta = 0.3i$, $R_s = 5$ Gsa/s, and $N_p = 32$ were selected for the comparison. The simulation results including the effects of A/D conversion (quantization) and noise are plotted in Fig. 13. The number of quantization bits was set to eight. We added white Gaussian noise (WGN) to emulate the noise effect in the simulation such that the received waveform had almost the same SNR as that in the experiment. To be specific, the average power spectral density of the noise level $\overline{N_0}$ in the simulation was matched with that in the experiment in the frequency domain after fitting the signal spectra. To match

the noise level, the spectrum of the experiment was obtained by computing the Fourier transform of the waveform acquired by the DSO. The estimation accuracy of the experiment was inferior to that of the ideal numerical simulations because of noise. However, the simulation results including the noise effect were almost the same as the experimental results. The limiting factor for the estimation accuracy was the noise effect and not the quantization effect, under the experimental conditions.

V. CONCLUSION

We evaluated the NFT-based CFO estimation method through numerical simulations and experiments. The NFT-based CFO estimation method achieved an estimation accuracy of less than 10 kHz when the time window size and sampling rate were $W = 6.4$ ns and $R_s = 20$ Gsa/s in the numerical simulations, respectively. When $R_s = 20$ Gsa/s, the estimation accuracy was better than that of the FFT-based CFO estimation in the range 0.4 ns $\leq W \leq 12.8$ ns. In addition, the estimation error was proportional to energy loss when the time window size W and sampling rate R_s were limited. Through experiments, a fine estimation accuracy below 1 MHz was achieved when $W = 12.8$ ns and $R_s = 5$ Gsa/s, although the accuracy was limited by the noise effect.

REFERENCES

- [1] A. Hasegawa and T. Nyu, "Eigenvalue communication," *IEEE/OSA J. Lightw. Technol.*, vol. 11, no. 3, pp. 395–399, Mar. 1993.
- [2] M. J. Ablowitz and H. Segur, *Solitons and the Inverse Scattering Transform*. Philadelphia, PA, USA: SIAM, 1981.
- [3] H. Terauchi and A. Maruta, "Eigenvalue modulated optical transmission system based on digital coherent technology," in *Proc. 10th Proc. Conf. Lasers Electro-Opt. Pacific Rim, 18th Opto-Electron. Commun. Conf./Int. Conf. Photon. Switching*, Kyoto, Japan, 2013, Paper WR2-5.
- [4] M. I. Yousefi and F. R. Kschischang, "Information transmission using the nonlinear Fourier transform, Part II: Numerical methods," *IEEE Trans. Inform. Theory*, vol. 60, no. 7, pp. 4329–4345, Jul. 2014.
- [5] S. K. Turitsyn et al., "Nonlinear Fourier transform for optical data processing and transmission: Advances and perspectives," *OSA Optica*, vol. 4, no. 3, pp. 307–322, Mar. 2017.
- [6] S. Hari, M. I. Yousefi, and F. R. Kschischang, "Multieigenvalue communication," *IEEE/OSA J. Lightw. Technol.*, vol. 34, no. 13, pp. 3110–3117, Jul. 2016.
- [7] T. Kodama, T. Zuiki, K. Mishina, and A. Maruta, "Hyper multilevel modulation based on optical eigenvalue multiplexing," in *Proc. Photon. Switching Comput.*, Limassol, Cyprus, 2018, Art. no. Th3C.4.

- [8] H. Takeuchi, K. Mishina, Y. Terashi, D. Hisano, Y. Yoshida, and A. Maruta, "Eigenvalue-domain neural network receiver for 4096-ary eigenvalue-modulated signal," in *Proc. Opt. Fiber Commun. Conf.*, San Diego, CA, USA, 2023, Art. no. Th3F.3.
- [9] S. T. Le, V. Aref, and H. Buelow, "Nonlinear signal multiplexing for communication beyond the Kerr nonlinearity limit," *Nature Photon.*, vol. 11, pp. 570–577, Sep. 2017.
- [10] T. Gui, T. H. Chan, C. Lu, A. P. T. Lau, and P.-K. A. Wai, "Alternative decoding methods for optical communications based on nonlinear Fourier transform," *IEEE/OSA J. Lightw. Technol.*, vol. 35, no. 9, pp. 1542–1550, May 2017.
- [11] R. T. Jones, S. Gaiarin, M. P. Yankov, and D. Ziber, "Time-domain neural network receiver for nonlinear frequency division multiplexed systems," *IEEE Photon. Technol. Lett.*, vol. 30, no. 12, pp. 1079–1082, Jun. 2018.
- [12] K. Mishina, S. Sato, Y. Yoshida, D. Hisano, and A. Maruta, "Eigenvalue-domain neural network demodulator for eigenvalue-modulated signal," *IEEE/OSA J. Lightw. Technol.*, vol. 39, no. 13, pp. 4307–4317, Jul. 2021.
- [13] L. Li, Z. Tao, S. Oda, T. Hoshida, and J. C. Rasmussen, "Wide-range, accurate and simple digital frequency offset compensator for optical coherent receivers," in *Proc. Opt. Fiber Commun. Conf.*, San Diego, CA, USA, 2008, pp. 1–3.
- [14] Optical Internet working Forum, Integrable Tunable Laser Assembly MSA, (OIF-ITLA-01.2), Jun. 2008.
- [15] Optical Internet working Forum, Micro Integrable Tunable Laser Assembly (OIF-MicroITLA-01.0), Sep. 2011.
- [16] K. Mishina, T. Maeda, D. Hisano, Y. Yoshida, and A. Maruta, "Combining IST-Based CFO compensation and neural network-based demodulation for eigenvalue-modulated signal," *IEEE/OSA J. Lightw. Technol.*, vol. 39, no. 23, pp. 7370–7382, Dec. 2021.
- [17] T. Nakagawa et al., "Non-data-aided wide-range frequency offset estimator for QAM optical coherent receivers," in *Proc. Opt. Fiber Commun. Conf. Expo. Nat. Fiber Opt. Eng. Conf.*, Los Angeles, CA, USA, 2011, Art. no. OMJ1.
- [18] M. Selmi, Y. Jaouen, and P. Ciblat, "Accurate digital frequency offset estimator for coherent PolMux QAM transmission systems," in *Proc. 35th Eur. Conf. Opt. Commun.*, Vienna, Austria, 2009, Art. no. P3.08.
- [19] Y. Cao, S. Yu, Y. Chen, Y. Gao, W. Gu, and Y. Ji, "Modified frequency and phase estimation for M-QAM optical coherent detection," in *Proc. 36th Eur. Conf. Opt. Commun.*, Trino, Italy, 2010, Art. no. We.7.A.1.
- [20] D. Zhao, L. Xi, X. Tang, W. Zhang, Y. Qiao, and X. Zhang, "Digital pilot aided carrier frequency offset estimation for coherent optical transmission system," *OSA Opt. Exp.*, vol. 23, no. 19, pp. 24822–24832, Sep. 2015.
- [21] Z. Zheng, X. Zhang, R. Yu, L. Xi, and X. Zhang, "Frequency offset estimation for nonlinear frequency division multiplexing with discrete spectrum modulation," *OSA Opt. Exp.*, vol. 27, no. 20, pp. 28223–28238, Sep. 2019.
- [22] T. Maeda, K. Mishina, D. Hisano, Y. Yoshida, and A. Maruta, "Soliton-assisted carrier frequency offset estimation in the eigenvalue domain," in *Proc. Int. Conf. Photon. Switching Comput.*, 2021, Art. no. Tu5A.5.
- [23] T. Maeda, K. Mishina, D. Hisano, and A. Maruta, "Experimental demonstration of CFO estimation in optical eigenvalue-domain," in *Proc. Conf. Lasers Electro- Opt.*, San Jose, CA, USA, May 2022, Art. no. JTh3B.11.
- [24] G. Agrawal, *Nonlinear Fiber Optics*, 5th ed., Cambridge, MA, USA: Academic Press, 2012.
- [25] A. Hasegawa and Y. Kodama, "Guiding-center soliton in optical fibers," *OSA Opt. Exp.*, vol. 15, no. 24, pp. 1443–1445, Dec. 1990.
- [26] A. Maruta, Y. Matsuda, H. Terauchi, and A. Toyota, "Digital coherent technology-based eigenvalue modulated optical fiber transmission system," in *Odyssey of Light in Nonlinear Optical Fibers: Theory and Applications*, K. Porsezian and R. Ganapathy, Eds. Boca Raton, FL, USA: CRC Press, 2015, Ch. 19, pp. 491–505.
- [27] Y. Terashi, D. Hisano, K. Mishina, Y. Yoshida, and A. Maruta, "Multi-eigenvalue demodulation using complex moment-based eigensolver and neural network," *IEEE/Optica J. Lightw. Technol.*, early access, Feb. 22, 2023, doi: [10.1109/OJLT.2023.3247775](https://doi.org/10.1109/OJLT.2023.3247775).
- [28] J. P. Gordon and H. A. Haus, "Random walk of coherently amplified solitons in optical fiber transmission," *OSA Opt. Lett.*, vol. 11, no. 10, pp. 665–667, Oct. 1986.

Takaya Maeda received the B.E. degree in 2021 in electrical, electronic, and information engineering from Osaka University, Osaka, Japan, where, he is currently working toward the M.E. degree.

Daisuke Hisano (Member, IEEE) received the B.E., M.E., and Ph.D. degrees in electrical, electronic, and information engineering from Osaka University, Osaka, Japan in 2012, 2014, and 2018, respectively. In 2014, he joined NTT Access Network Service Systems Laboratories, Yokosuka, Japan. Since 2018, he has been an Assistant Professor with the Department of Information and Communication Technology, Division of Electrical, Electronic, and Information Engineering, Graduate School of Engineering, Osaka University. His research interests include optical-wireless converged networks, optical communication, and all-optical signal processing. He is a member of IEICE, Japan.

Yuki Yoshida (Member, IEEE) received the B.S., M.S., and Ph.D. degrees in informatics from Kyoto University, Kyoto, Japan, in 2004, 2006, and 2009, respectively. From 2009 to 2016, he was an Assistant Professor with Osaka University, Osaka, Japan. Since 2016, he has been with Network Research Institute, National Institute of Information and Communications Technology, Tokyo, Japan, where he is currently a Research Manager. He is also a Visiting Associate Professor with Osaka University. His research interests include digital signal processing for optical/wireless communications, optical/wireless access, and optical-wireless convergence. He is a Member of IEICE, Japan.

Akihiro Maruta (Member, IEEE) received the B.E., M.E., and Ph.D. degrees in communication engineering from Osaka University, Osaka, Japan in 1988, 1990, and 1993, respectively. He joined the Department of Communications Engineering, Osaka University, in 1993. Since 2016, he has been a Professor with the Department of Information and Communication Technology, Osaka University. His research interests include optical fiber communication systems and all-optical signal processing. He is a Member of IEEE Photonics Society and Optical Society of America (OSA), and Senior Member of IEICE, Japan.

Ken Mishina (Member, IEEE) received the B.E., M.E., and Ph.D. degrees in electrical, electronic, and information engineering from Osaka University, Osaka, Japan, in 2005, 2007, and 2012, respectively. In 2007, he joined Shimadzu Corporation, Kyoto, Japan. Since 2018, he has been an Associate Professor with the Department of Information and Communication Technology, Division of Electrical, Electronic, and Information Engineering, Graduate School of Engineering, Osaka University. His research interests include optical fiber communication systems, all-optical signal processing and photovoltaics. He is a member of IEEE Photonics Society and IEICE, Japan.